

# Investigation of earthquake signatures on the Ionosphere over Europe

Haris Haralambous<sup>1</sup>, Christina Oikonomou<sup>1</sup>, Buldan Muslim<sup>2</sup>

<sup>1</sup>Frederick Research Center  
*Filokyprou St.7, Palouriotissa, Nicosia, 1036, Cyprus*

<sup>2</sup>Space Science Center, Indonesian National Institute of Aeronautics and Space  
*Jl. Dr. Junjunan 133, Bandung, 4017, Indonesia*

## ABSTRACT

We present preliminary results of a research project that concerns the investigation of the lithosphere-atmosphere-ionosphere interaction with respect to earthquake events by applying two different techniques, Cross-Correlation Analysis and Spectral Analysis on two ionospheric characteristics, Total Electron Content (TEC) and critical frequency of F2 layer. The analysis is conducted for certain seismic events that took place at Southern Europe during the period 1998-2013 with their magnitude ranging from 5.9 to 7.2. The aim is to identify possible ionospheric precursory phenomena and examine their main characteristics.

## 1. INTRODUCTION

In the last two decades, the link between seismic activity and ionospheric perturbations related to earthquake precursory phenomena has acquired significant attention. Possible earthquake precursors have been identified including ground deformations, radon/helium emissions, crustal stress, atmospheric thermal anomalies (Pulinets et al., 2004). Gas emissions prior to an earthquake cause ionisation of the neutral atmosphere above the epicenter and thus the generation of anomalous electric field that penetrates the ionosphere leading to large-scale positive and negative anomalies of electron concentration in the vicinity of the epicenter. This electric field is not restricted only to the epicenter, but covers an area that is a function of the earthquake magnitude named as earthquake preparation zone. In addition, Atmospheric Gravity Waves (AGW) are generated by pre-seismic activity of emanating gases. The most widely known long wavelength perturbations are travelling ionospheric disturbances (TIDs) which are associated to AGW (Artru et al., 2005) and also infrasonic waves propagating upwards, amplified by the exponential density decrease of the atmosphere (Artru et al., 2004). It has been statistically proved that ionospheric precursors are observed between 12 days to a few hours prior to the earthquake and that earthquakes should exceed the magnitude of 5 in order to provoke ionospheric disturbances. The duration of a seismically induced ionospheric deviation is short about 4–6 hours being compared with perturbations caused by geomagnetic storms (Pulinets et al., 2004).

The aim of this study is to investigate the possible correlation of ionospheric perturbations prior to earthquake with seismic activity, in order to provide tangible evidence to justify a lithosphere-atmosphere-ionosphere interaction, by applying two different analysis techniques, Cross-

Correlation Analysis and Spectral Analysis to GNSS and Ionosonde observations over the European area for certain earthquake events that took place during the period 1998-2013.

## 2. DATA AND METHOD OF ANALYSIS

The seismic events were selected from the earthquake catalog provided by the United States Geological Survey's (USGS) Earthquake Hazards Program so as to satisfy the criteria of having magnitude ( $M_w$ ) ranging from 5.9 to 7.2 and of existing observational data availability during and prior to earthquake events for the period 1998-2014 and over the European area. This interval is chosen based on the fact that modern digital ionosonde development and large scale GNSS network deployment was realised around 1998. Table 1. shows the selected earthquake events as well as their main characteristics.

In order to detect possible ionospheric disturbances prior to earthquakes, total electron content (TEC) obtained from dual-frequency phase and code measurements made by GNSS receivers (Table 1) located in Europe and belonging to EUREF Permanent networks, as well as hourly observations of the critical frequency of F2 ionospheric layer (foF2) provided by four ionosondes at Rome, San Vito, Athens and Nicosia were employed. Figure 1 presents maps of the GNSS stations and the ionosonde stations along with the epicenters of the earthquakes analysed in this study. In order to calculate vertical TEC (vTEC) we have processed RINEX files from the selected GNSS stations with a calibration algorithm (Ciraolo, 1993). This processing technique assumes ionospheric thin shell model (located at 350km of altitude) to obtain vTEC from slant total electron content (sTEC) at the Ionospheric Pierce Point (IPP). It should be mentioned that foF2 measurements were manually scaled using the SAO-explorer software (Sao Explorer, Interactive Ionogram Scaling Technologies, <http://ulcar.uml.edu/SAO-X/SAO-X.html>; (Reinisch et al., 2004) developed by the University of Lowell Massachusetts, Center for Atmospheric Research for quality control.

**Table 1.** List of earthquakes, their characteristics and GNSS stations used for this study.

No of Earthq.	$M_w$	Date time (UT)	R (km)	GNSS stations Inside preparation area	GNSS stations Outside preparation area	Lat (°)	Lon (°)	Depth (Km)	Region
E1	7.2	11/12/1999 16:57	1247	ANKR	NOTO, AQU1	40.78	31.21	10	western Turkey
E2	6.9	2/14/2008 10:09	927	TUC2	AQU1, NICO	36.50	21.67	29	southern Greece
E3	6.5	2/14/2008 12:08	624	TUC2	AQU1, NICO	36.35	21.86	28	southern Greece
E4	6.4	6/8/2008 12:25	565	AUT1, TUC2	ANKR	37.96	21.53	16	southern Greece
E5	6.3	4/6/2009 1:32	512	AQU1	AUT1, SOFI	42.33	13.33	8.8	central Italy
E6	6.2	6/15/2013 16:11	463	TUC2	ANKR, NICO, NOT1	34.45	25.04	10	Crete, Greece
E7	6.2	1/6/2008 5:14	463	TUC2	NICO, AQU1	37.22	22.69	75	southern Greece
E8	6	4/1/2011 13:29	380	TUC2	DEVA, MOSE	35.66	26.56	59.9	Crete, Greece

First, the cross-correlation technique was applied for all seismic events and for both vTEC data with 5 minutes resolution and hourly foF2 data. For this purpose, the preparation area was defined for each earthquake by estimating its radius using the following equation developed by (Dobrovolsky et al., 1979):  $\rho = 10^{0.43M} \text{ km}$ , where M is the magnitude ( $M_w$ ) of the earthquake. In this technique two measurement points are used: one located inside the earthquake preparation area and

the other outside. Since ionospheric variability induced by seismic activity is generally lower than those variations related to geomagnetic storms, it is masked by storm-time variations. In order to overcome this problem the two sites should be in the same or very close geomagnetic latitude so that ionospheric variations registered at both sites exhibit similar behavior during quiet and disturbed geomagnetic conditions. Therefore, their correlation coefficient will be high. On the contrary, during seismic activity their correlation coefficient is expected to drop since the station closer to epicenter (inside the preparation area) will be more sensitive to seismic variations than the station outside the preparation area. In addition, the longitude of the two sites should not be so different, as ionosphere is local time dependent.

The daily cross-correlation coefficient between ionospheric variations ( $\nu$ TEC, foF2 variations) observed at the site located inside and the site located outside the preparation zone was assessed. For each site, the auto-correlation coefficient was also performed, by estimating the daily auto-correlation coefficient between one day and the next day. Any drop of the coefficient detected at the auto-correlation of the station measurements inside the preparation zone will be transferred at the cross-correlation coefficient only if it is induced by seismic activity, while the drops of auto-correlation coefficient caused by geomagnetic storms are not transferred at the cross-correlation coefficient variations (Pulinets et al., 2004). The GNSS receiver stations inside and outside the preparation area are recorded at Table 1.

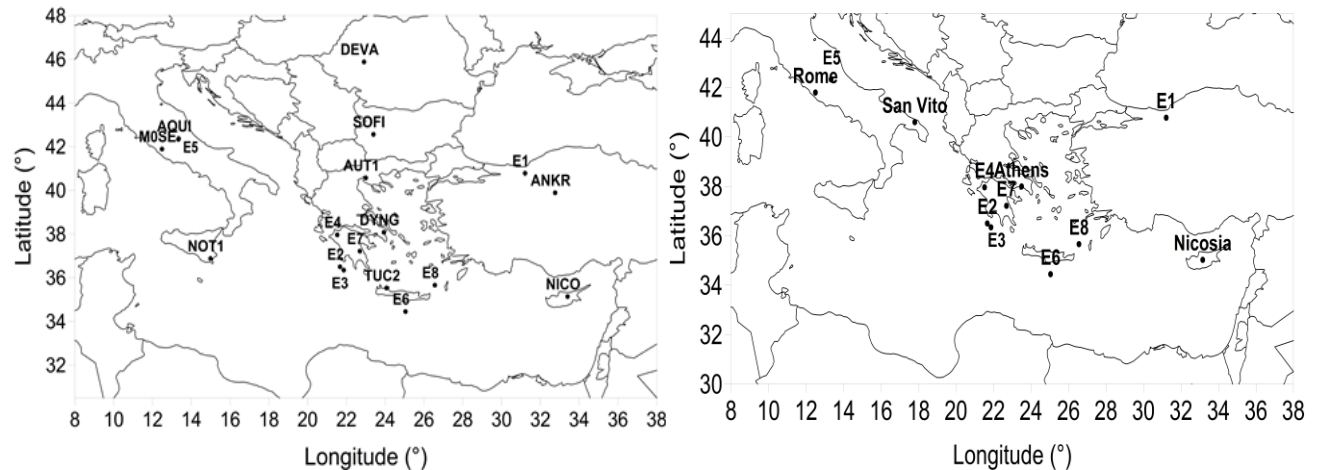


**Figure 1.** Map of selected European GNSS receivers (left panel) and map of selected Ionosonde stations (right panel). The epicenters of the examined earthquakes as listed at Table 1 are also depicted at both maps symbolized as E1, E2, E3, E4, E5, E6, E7, and E8.

Although geomagnetic storm effects on ionospheric variability are excluded by the use of cross-correlation analysis, there are still ionospheric variations in the signals of both sites caused by unknown sources that can be uncorrelated. For this reason, we applied also spectral analysis. For this method, we have used differential TEC, described as the difference of sTEC measurement between two successive satellite epochs. The sTEC was estimated using an algorithm developed by (Muslim et al., 2013) that defines sTEC following the equations given by (Gao et al., 2002). Since we are searching possible large-scale ionospheric precursors induced from anomalous electric field or AGWs caused by gas emissions several days prior to earthquakes we performed spectral analysis in order to detect high fluctuations of differential sTEC with period of oscillation up to 30 minutes. The amplitude of these oscillations was also estimated.

### 3. RESULTS

In Figures 2 to 8 daily variations of cross- and auto- correlation coefficients both for vTEC and foF2 variations are depicted for all examined seismic events at the interval fifteen days prior, during and up to two days after the earthquake. In the same figures the disturbed geomagnetic conditions during the events under investigation are denoted according to the ranking described at the geomagnetic bulletins provided by the National Geophysical Data Center (NGDC) (<https://www.ngdc.noaa.gov/>). The five most active days from the most (D1) to least disturbed (D5) are shown. As it can be seen, the earthquakes of the 6<sup>th</sup> January 2008 and 1<sup>st</sup> April 2011 took place during geomagnetically disturbed conditions. Inspection of all seismic events reveals that the drop of the TEC cross-correlation coefficients coincides with the foF2 cross-correlation coefficients in all cases, which is in agreement with (Artru et al., 2005). The cross-correlation coefficient appears to fall, in general, 12, 7, 5, 2 days before the earthquake or even at the day of earthquake as it had happened during the 6<sup>th</sup> of April 2009 earthquake at L' Aquila, Italy. The drop in the cross-correlation coefficient that was observed two days before this earthquake, as well as the drop eight days before the earthquake at 1<sup>st</sup> of April 2011 were also detected in (Tsolis et al., 20095) where the correlation analysis at foF2 denoised signals was applied.

The Spectral Analysis was conducted for each seismic event and for differential TEC during the dates of earthquakes, the days where reduction of cross-correlation coefficient was noticed and during a reference day for each event where no ionospheric or geomagnetic disturbances were observed. Therefore, comparison of TEC fluctuations during these dates was possible. The results only for the earthquake with the largest magnitude (Mw=7.2) that took place at Ankara during 12<sup>th</sup> November 1999 are presented here. Figures 9 and 10 show the fluctuations of differential TEC and the power spectrum of a normalized amplitude of fluctuation which is directly proportional to the real amplitude during certain times (UT) of two days (7<sup>th</sup> and 11<sup>th</sup> November 1999) characterized by high reduction of cross-correlation coefficient. Since during these days a moderate geomagnetic storm was under development the period of differential TEC oscillation was chosen to be up to 30 minutes, so that fluctuations induced by geomagnetic storms which have larger than 30 minutes period of oscillation to be excluded. As it can be seen at both figures, the Ionospheric Pierce Points (IPP) of all satellites except satellite PRN 24 were located inside the preparation zone and most of them close to the earthquake epicenter. The TEC variations produced by measurements of these satellites and the GPS receiver located at Bucharest are periodic around a certain hour at both days, apart from satellite PRN24 which is far from the epicenter. The highest differential TEC fluctuation was observed at both days by the satellite whose IPP was located closer to the earthquake epicenter (PRN 2). In the same figures the power spectrum demonstrates an enhancement of amplitude, whereas the period of TEC oscillations is around 15 minutes.

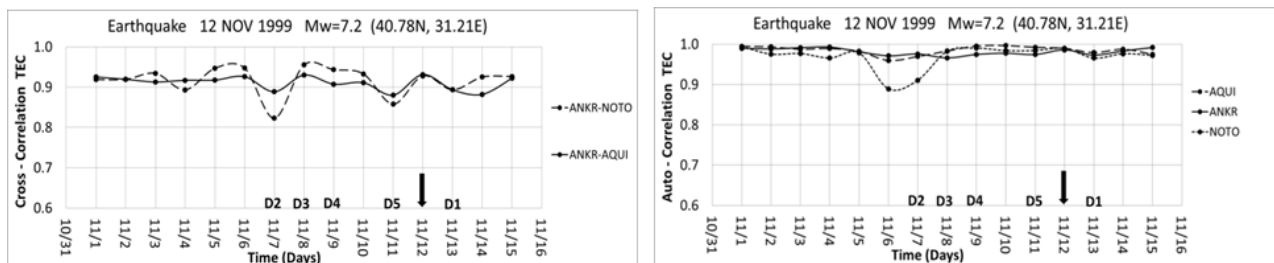


**Figure 2.** Left panel: cross-correlation coefficient for vTEC signals for the selected stations for the earthquake of 12<sup>th</sup> November 1999. Right panel: auto-correlation coefficient for the same stations. Black arrow indicates the day of earthquake. Geomagnetically disturbed days are denoted with Di (i=1, 2, 3, 4, 5) following the NCDC ranking criteria.

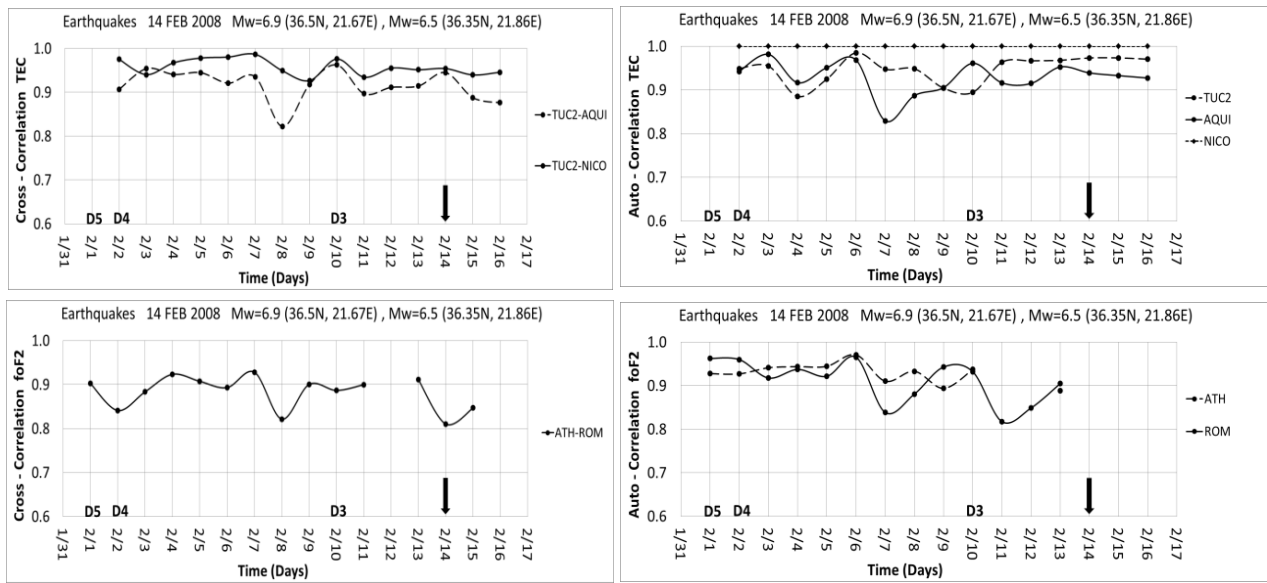


**Figure 3.** Upper left panel: cross-correlation coefficient of  $vTEC$  for the selected stations for the earthquake of 14<sup>th</sup> February 2008. Upper right panel: auto-correlation coefficient of  $vTEC$  for same stations. Lower left panel: cross-correlation coefficient of foF2 for the selected stations for the same earthquake. Lower right panel: auto-correlation coefficient of foF2 for same stations. Black arrow indicates the day of earthquake. Geomagnetically disturbed days are denoted with Di ( $i=1, 2, 3, 4, 5$ ) following the NCDC ranking criteria.

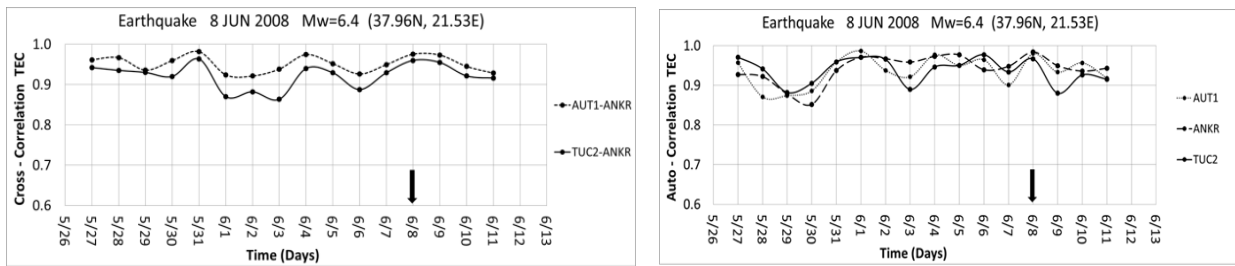


**Figure 4.** Same as figure 2, but for the earthquake of 8<sup>th</sup> June 2008.

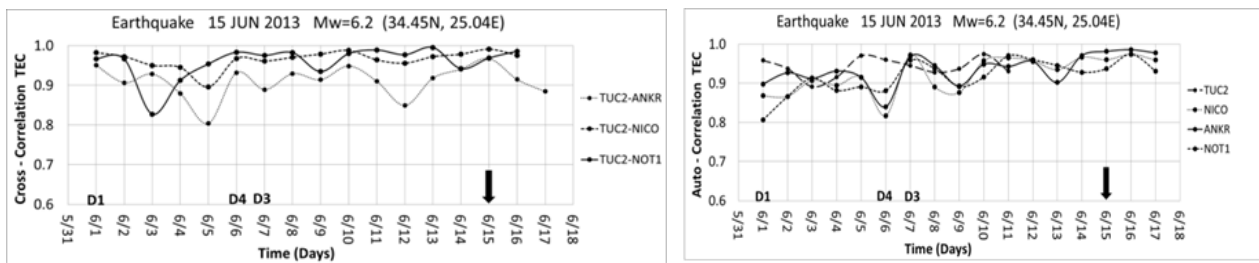


**Figure 5.** Same as figure, 2 but for the earthquake of 15<sup>th</sup> June 2013.

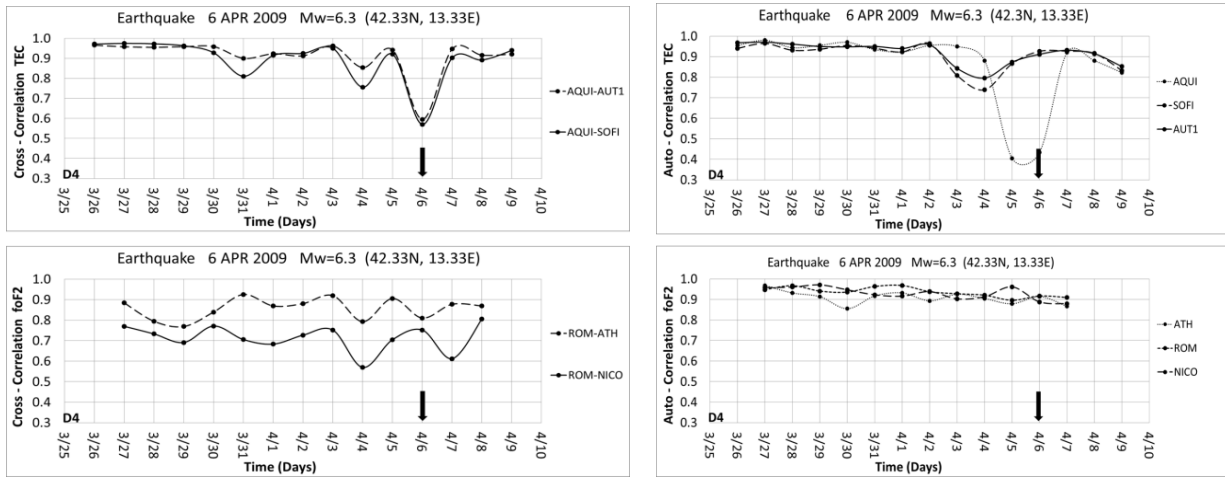


Figure 6. Same as figure 3, but for the earthquake of 6<sup>th</sup> April 2009.

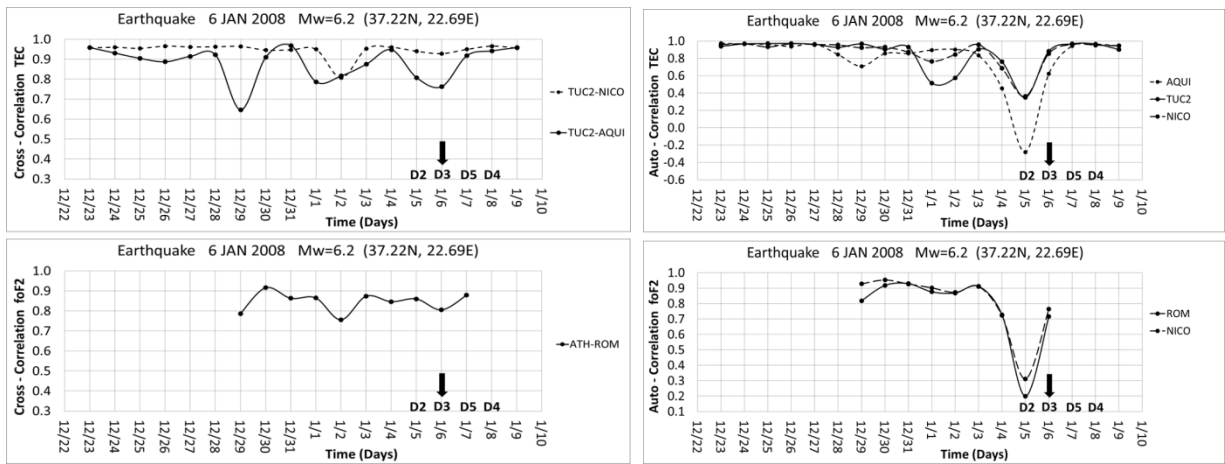


Figure 7. Same as figure 3, but for the earthquake of 6<sup>th</sup> January 2008.

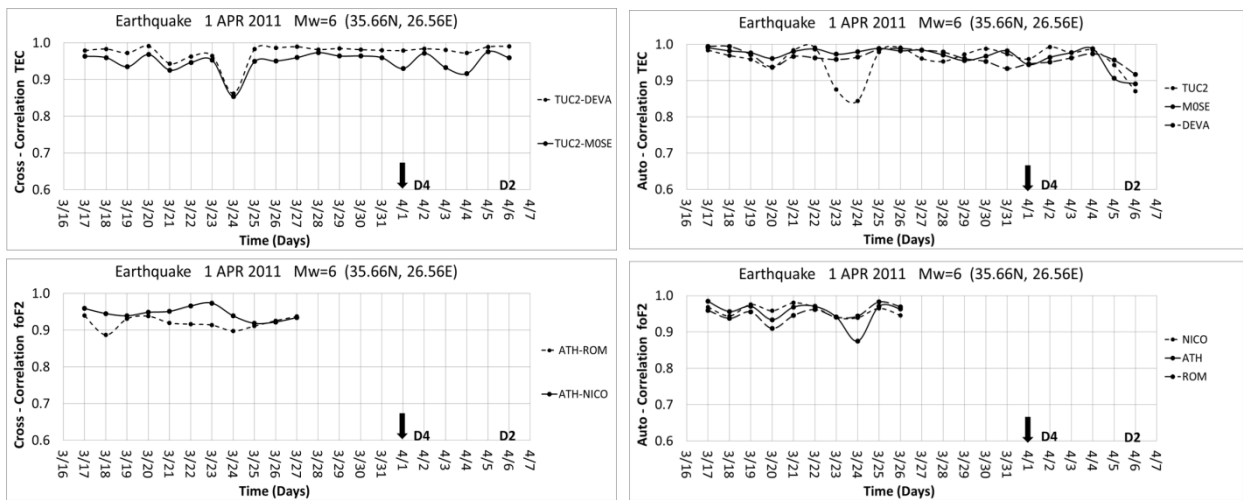
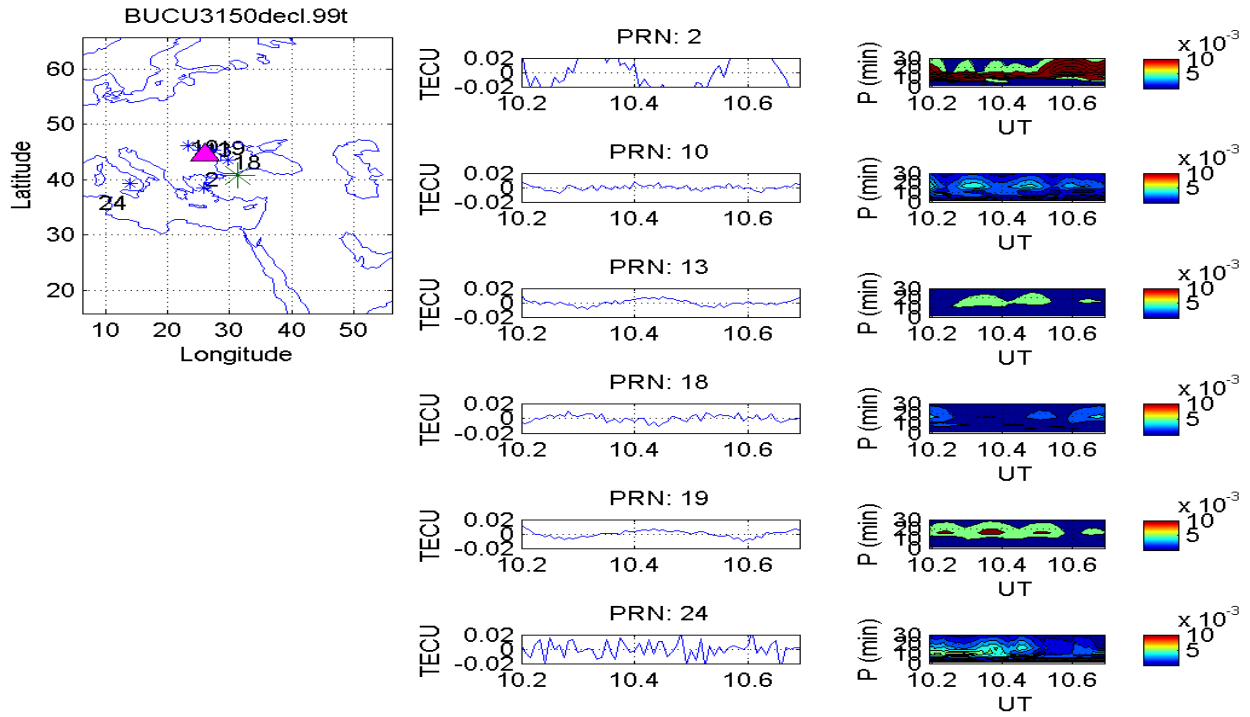
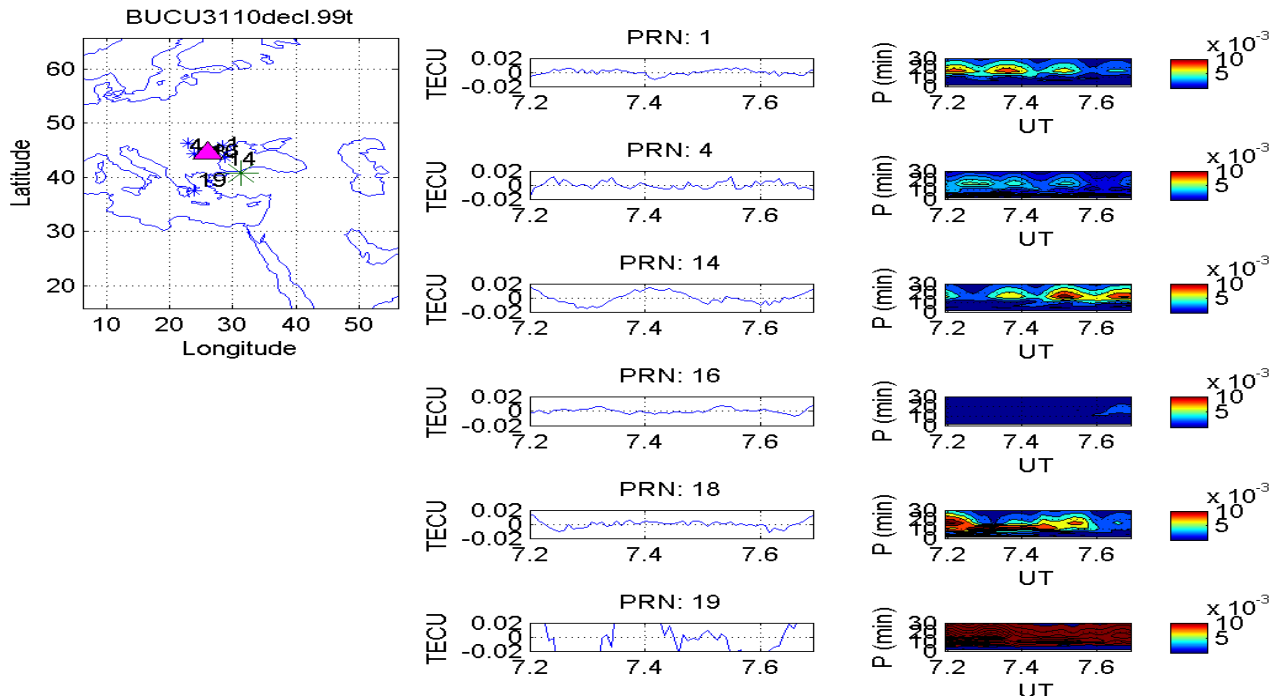


Figure 8. Same as figure 3, but for the earthquake of 1<sup>st</sup> April 2011.



**Figure 9.** Fluctuations of differential TEC (middle panels) obtained from measurements of 6 satellites passing over the preparation zone around hour 7 UT of 7<sup>th</sup> November 1999 where large drop of cross-correlation coefficient was found. The power spectrum of the normalized amplitude is also shown (right panels). Map shows the number and position of satellites (blue asterisks), the position of the GPS receiver (pink triangle) at the same date, and the epicenter (green asterisk) of the earthquake at 12<sup>th</sup> November 1999.



**Figure 10.** Same as figure 9, for 11<sup>th</sup> November 1999 where drop of cross-correlation coefficient was noted.

## 4. CONCLUSIONS

The application of Cross-Correlation Analysis for  $v$ TEC and foF2 variations for eight seismic events that occurred at southern Europe during the period 1999-2013 has shown that ionospheric precursory phenomena can be observed from few hours up to 12 days before the earthquake. Spectral Analysis applied for maximum period of TEC oscillation up to 30 minutes is capable of distinguishing seismically induced TEC fluctuation anomalies from those generated by storms. Since ionospheric perturbations induced by earthquakes are masked by ionospheric anomalies that are caused by geomagnetic storms, the simultaneous utilization of these techniques provides more safe conclusions in terms of identifying ionospheric precursors.

## ACKNOWLEDGEMENTS

This paper is funded by the project “Investigation of earthquake signatures on the ionosphere over Europe- $\Delta$ IAKPATIKEΣ/KY-POY/0713/37” which is co-financed by the Republic of Cyprus and the European Regional Development Fund (through the  $\Delta$ ΕΣΜΗ 2009-2010 of the Cyprus Research Promotion Foundation).

## REFERENCES

- Artru, J., Ducic, V., Kanamori, H., Lognonn e, P., & Murakami, M. (2005). Ionospheric detection of gravity waves induced by tsunamis, *Geophys. J. Int.*, 160, 840-848.
- Artru, J., Farges, T., and Lognonn e, P. (2004). Acoustic waves generated from seismic surface waves: propagation properties determined from doppler sounding observation and normal-modes modeling, *Geophys. J. Int.*, 158, 1067-1077.
- ] Ciraolo, L. (1993). Evaluation of GPS L2-L1 biases and related daily TEC profiles, in: *Proc. of the GPS/Ionosphere Workshop*, 90–97, Neustrelitz.
- Dobrovolsky, I. R., Zubkov, S. I., and Myachkin, V. I. (1979). Estimation of the size of earthquake preparation zones, *Pageoph.*, 117, 1025–1044.
- Gao, Y., Liu, Z.Z. (2002). Precise ionosphere modeling using regional GPS network data. *J. of Global Pos. Sys.*, 28-24.
- Muslim, B., Efendi, J., and Suryanal, D.R. (2013). Developing near real time TEC computation system from GPS data for improving spatial resolution of ionospheric observation over Indonesia. *Proceeding of 1st International Seminar on Space Science and Technology*, Serpong, Indonesia, Dec. 3, 2013.
- Pulinets S.A. and Boyarchuk K.A. (2004). *Ionospheric precursors of earthquakes*, Springer, Berlin.
- Reinisch, B.W., Galkin, I.A., Khmyrov, G., Kozlov, A., Kitrosser, D.F. (2004). Automated collection and dissemination of ionospheric data from the digisonde network. *Adv. Radio Sci.* 2 (1), 241–247.
- Tsolis, G.S., and Xenos, T.D. (2009). Seismo-ionospheric coupling correlation analysis of earthquakes in Greece, using Empirical Mode Decomposition. *Nonlin. Processes Geophys.*, 16, 123–130.